Journal of Power Sources 183 (2008) 761–765

Contents lists available at ScienceDirect

Journal of Power Sources

journal homepage: www.elsevier.com/locate/jpowsour

Short communication

Synthesis and electrochemical properties of $Li(Ni_{0.8}Co_{0.1}Mn_{0.1})O_2$ cathode material: *Ex situ* structural analysis by Raman scattering and X-ray diffraction at various stages of charge–discharge process

José J. Saavedra-Arias, Naba K. Karan, Dillip K. Pradhan, Arun Kumar, Santander Nieto[1], Reji Thomas, Ram S. Katiyar*

Department of Physics and Institute for Functional Nanomaterials, University of Puerto Rico, PO Box 23343, San Juan, PR 00931-3343, USA

ARTICLE INFO

Article history:
Received 4 March 2008
Received in revised form 24 May 2008
Accepted 26 May 2008
Available online 3 June 2008

Keywords:
Li-ion rechargeable battery
Cathode
Raman scattering
XRD
Charge–discharge

ABSTRACT

$Li(Ni_{0.8}Co_{0.1}Mn_{0.1})O_2$ cathode materials were synthesized by solid-state reaction route. Single-phase layer structure with hexagonal unit cell having $R\bar{3}m$ symmetry was obtained and the average particle size was around 6 μm. Electrochemical studies showed single redox reaction and a maximum charging capacity of ~140 mAh g^{-1} was obtained. *Ex situ* structural studies by X-ray diffraction and Raman scattering at various stages of charging and discharging showed that the host layered structure is maintained throughout the electrochemical lithiation–delithiation processes in the 3–4.5 V range with systematic change in the lattice parameters. First discharge capacity was 132 mAh g^{-1} and the capacity retention was ~86% after 20 charge–discharge cycles.

1. Introduction

Since its introduction in the consumer market at the beginning of 1990s by Sony Corporation 'Li-ion rechargeable battery' and '$LiCoO_2$ cathode' is an inseparable couple for highly reliable practical applications. However, a separation is inevitable as Li-ion rechargeable battery industry demand more and more from this well serving cathode. This cathode material has a practically usable capacity around 100–150 mAh g^{-1} only (half of the theoretical capacity, ~270 mAh g^{-1}), as the structural and chemical stability is big concern if one extracts more than half of Li from $LiCoO_2$ [1–3]. Cost, safety and environmental concerns along with higher energy and power requirements became prominent issues as consumer electronic devices demand increased manifold over the last decade. This made Li-ion battery as a common portable energy source and the replacement of Co partially or completely by other environmentally benign, cheap elements is of great practical importance. Some of the candidate materials considered to replace $LiCoO_2$ are: $LiNiO_2$ [4], $LiMnO_2$ [5], $LiMn_2O_4$ [6] and $LiFePO_4$ [7]. However, each of these candidate materials has its own disadvantages, e.g. layered $LiNiO_2$ is not having an electrochemically stable structure in terms of the operating voltage range (three phase transitions in the 3–4.5 V range); $LiMnO_2$ suffers from structural stability during electrochemical cycling (it changes from the layered to spinel structure after repeated charge–discharge cycles); a moderate capacity (~120 mAh g^{-1}) and severe capacity fading especially at elevated temperatures ~50 °C occurs in $LiMn_2O_4$; the poor electronic conductivity, which restricts the rate capability for $LiFePO_4$. The practical solutions to these problems ensure advancement of Li-ion rechargeable battery technologies to meet the future demands of the portable energy sector, which are mainly driven by smaller, faster and cheaper alternatives. However, to meet the conservative requirement of the battery industry (delays the new material opening), a direct and commonly adopted composite material (weakness of one is compensated by the strength of the other) based on the above-mentioned materials may be of great interest. This compromising idea is not novel to the battery community as cation ordering between Ni, Mn and Co ions in the lattice were recently discussed [8,9]. In this case, stabilization of the structure occurs by virtue of strain energy minimization of the lattice containing cations of different sizes. Due to these reasons an alternate layered Li-based cathode material based on $Li(Ni_xCo_yMn_{1-x-y})O_2$ is of great importance.

* Corresponding author. Tel.: +1 787 751 4210; fax: +1 787 764 2571.
E-mail addresses: jsaavedr@gmail.com (J.J. Saavedra-Arias), rkatiyar@uprrp.edu (R.S. Katiyar).
[1] School of Science and Technology, University of Turabo, Gurabo, PR 00778-3030, USA.

0378-7753/$ – see front matter © 2008 Elsevier B.V. All rights reserved.
doi:10.1016/j.jpowsour.2008.05.068

Since the interesting observation of high discharge capacity with $Li(Ni_{1/3}Co_{1/3}Mn_{1/3})O_2$ material in 2001 by Ohzuku and Makimura [10] enormous research on the layered cathode materials based on $Li(Ni_xCo_yMn_{1-x-y})O_2$ with various values of x and y have been reported in the literature [11–14]. The increase of Ni in $Li(Ni_xCo_yMn_{1-x-y})O_2$ reduces the cost. Additionally, with Ni it is reported that electrolyte decomposition at the end of the charge potential can be avoided and improve specific capacity [15,16]. In this paper, the synthesis of $Li(Ni_{0.8}Co_{0.1}Mn_{0.1})O_2$ material and structural changes at different stages of electrochemical process are discussed.

2. Experimental details

$Li(Ni_{0.8}Co_{0.1}Mn_{0.1})O_2$ was prepared by solid-state reaction between Li_2O (Alfa Aesar 99.95%), Ni(II)O (Alfa Aesar 99%), $Co_3(II,III)O_4$ (Alfa Aesar 99.7%) and $Mn(IV)O_2$ (Alfa Aesar 99.9%). Stoichiometric ratios of these reagent mixtures were first ball milled for 24 h in isopropanol media. The resulting mixture was dried at ~60 °C and subsequently fired at 450 °C for 4 h in air. Finally, the powder was calcined at various temperatures. The structure of the synthesized powder was determined by X-ray diffraction using Cu Kα radiation (Siemens D5000). Raman-scattering data were obtained using a T64000 spectrometer equipped with a triple-grating monochromator and a Coherent Innova 90C Ar^+-laser at 514.5 nm. The measurements were performed with a micro-Raman option employing normal backscattering geometry and a liquid N_2-cooled charge coupled device (CCD). Very low power (~0.2–0.4 mW) was used to ensure that the samples were not burnt during the laser exposure. The spectral resolution was typically less than 1 cm^{-1}. The electrochemical properties of the synthesized powder were carried out in two electrode CR2032 type coin cell configuration using liquid electrolyte consisting of $LiPF_6$ (1 M) dissolved in 1:1 (by weight) mixture of ethylene carbonate (EC) and dimethyl carbonate (DMC). The working electrode was prepared by mixing calcined powder, polyvinylidine fluoride, and carbon black in 80:10:10 weight ratio [17]. A slurry was prepared using *N*-methyl pyrrolidone (NMP) as solvent and was spread on Al foil and kept for drying at about 80 °C for 24 h. Li metal foil was used as anode and Celgard 2400 was used as separator between anode and cathode. The coin cell was assembled in Ar atmosphere inside a glove box (MBraun). The electrochemical measurements were performed on a computer controlled potentiostat/galvanostat system (consisting a PCI4/750 controller and PHE 200 software [Gamry Instrument]). The cyclic voltammograms were recorded at a scan speed of 0.02–0.1 mV s^{-1} in the voltage range 3–4.5 V and the charge discharge measurements were done in the voltage range 3–4.5 V at room temperature. For *ex situ* XRD and Raman measurements, the cells were disassembled inside the glove box and the cathode was rinsed repeatedly with DMC and finally dried.

3. Results and discussion

X-ray diffraction patterns of the $LiNi_{0.8}Co_{0.1}Mn_{0.1}O_2$ powder calcined at various temperatures in air for 48 h (700–1000 °C) are shown in Fig. 1. At lower calcination temperatures (≤800 °C), the material was diphasic, presence of additional phase with layered structure was observed and the extra peak around 22° in XRD pattern of this impurity phase matches with Li_2MnO_3. However, single-phase structure with layered structure was obtained with calcinations in air at a temperature ≥900 °C for 48 h. All the diffraction peaks were indexed based on a hexagonal unit cell (α-$NaFeO_2$ type layered structure) with space group $R\bar{3}m$ [18]. The narrowness of the diffraction lines indicates good crystallinity and bigger grain sizes at calcinations temperatures ≥900 °C. It is also clear that both

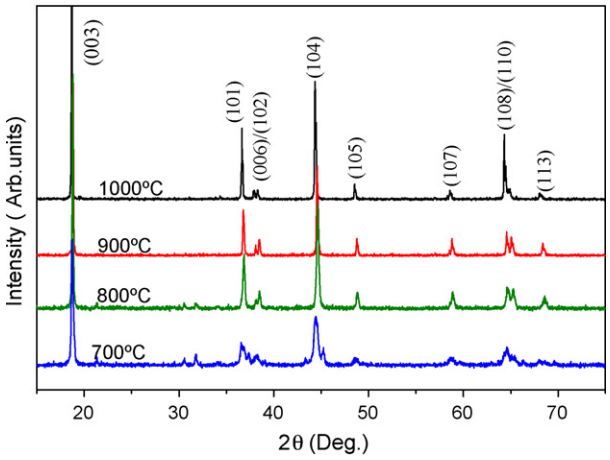

Fig. 1. XRD patterns of $LiNi_{0.8}Co_{0.1}Mn_{0.1}O_2$ calcined at various temperatures. The reflections matched well with the α-$NaFeO_2$ pattern with space group ($R\bar{3}m$).

double-peak (0 0 6)/(1 0 2) and (1 0 8)/(1 1 0) splits up well, which suggests good layered character of the synthesized powder [14,19]. Rietveld refinement of the XRD resulted in 3.5% (atomic) cation exchange (Ni^{2+} in Li^+ site) was. The cation intermixing of Li^+ and Ni^{2+} is, in general, very much dependent on synthesis route. The present value of cation exchange is comparable to the reported values for layered structure having similar compositions [20].

Morphology of the powder was observed with scanning electron microscope and Fig. 2 shows the SEM pictures of 900 °C and 1000 °C calcined $LiNi_{0.8}Co_{0.1}Mn_{0.1}O_2$ powder. Average particle size was around 5–8 μm in the case powders calcined at 900 °C (Fig. 2a), where as in the case of 1000 °C calcined powders (Fig. 2b), particle size increased many fold with wide grain-size distribution; suggestive of grain growth due to particle coalition at 1000 °C. Finer and uniform grain size distribution of the material is preferred for the cathode application and hence 900 °C calcined powder was selected for the electrochemical test. Smaller particle sizes (50–200 nm) may ensure shorter diffusion length for Li^+ that will improve the reversible capacity [21]. The particle size of the cathode material considered here was very high (5–8 μm) to have any positive influence on the reversible capacity. Since, we are interested in the structural changes of the cathode material upon electrochemical cycling, this important step was overlooked. Further, the stoichiometry of the prepared composition has been verified using EDAX analysis (not shown here). Since it is not practically possible to calculate the percentage of lithium present in the synthesized compound by applying EDAX, the stoichiometry of Co, Mn and Ni were examined. In the prepared composition atomic concentrations of Ni, Co and Mn were present in the ratio 77:12:9.

The cyclic voltammograms at room temperature with various scan rates (0.1 mV s^{-1}, 0.05 mV s^{-1} and 0.02 mV s^{-1}) in the voltage range 3–4.5 V are shown in Fig. 3a. All the curves have only one anodic and one cathodic peak, and hence only one electrochemical reaction and no structural transitions exist from hexagonal to monoclinic [22,19]. Moreover, the current peak is more separated for high scan rate and slowly the separation reduced as the scan rate reduced along with the lowering of the peak height with slower scan rate. If the electron transfer processes were 'slow' (relative to the voltage scan rate) this kind of behavior is observed in the electrochemical system. This along with the rounded behavior of cathodic and anodic peaks in the present case suggest to a quasi-reversible electron transfer process [23–25]. Galvanostatic charge–discharge profile for the first cycle is shown in Fig. 3b. First charge and discharge capacities in the voltage range 3.0–4.5 V were

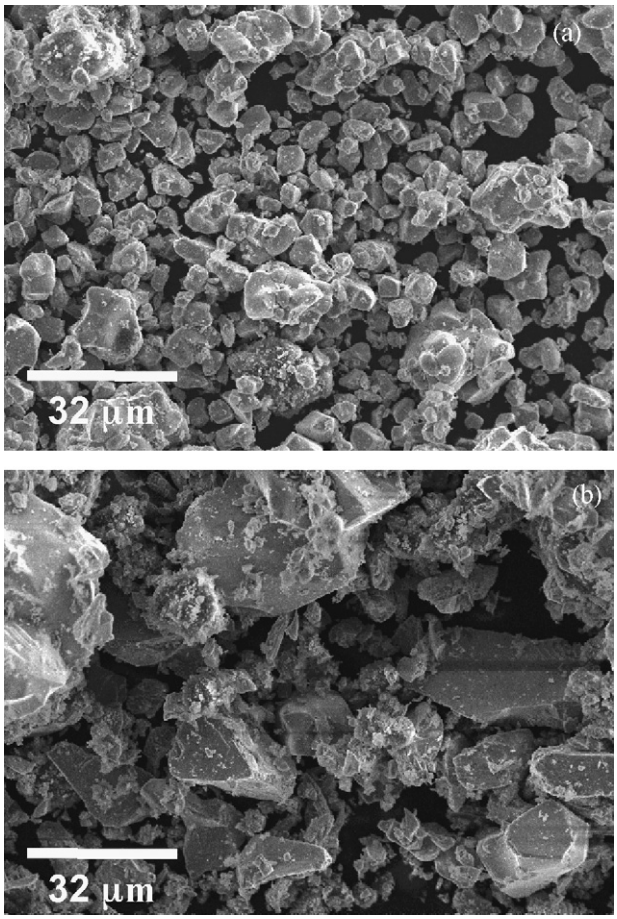

Fig. 2. Scanning electron micrograph of $LiNi_{0.8}Co_{0.1}Mn_{0.1}O_2$ calcined powder: (a) 900 °C and (b) 1000 °C.

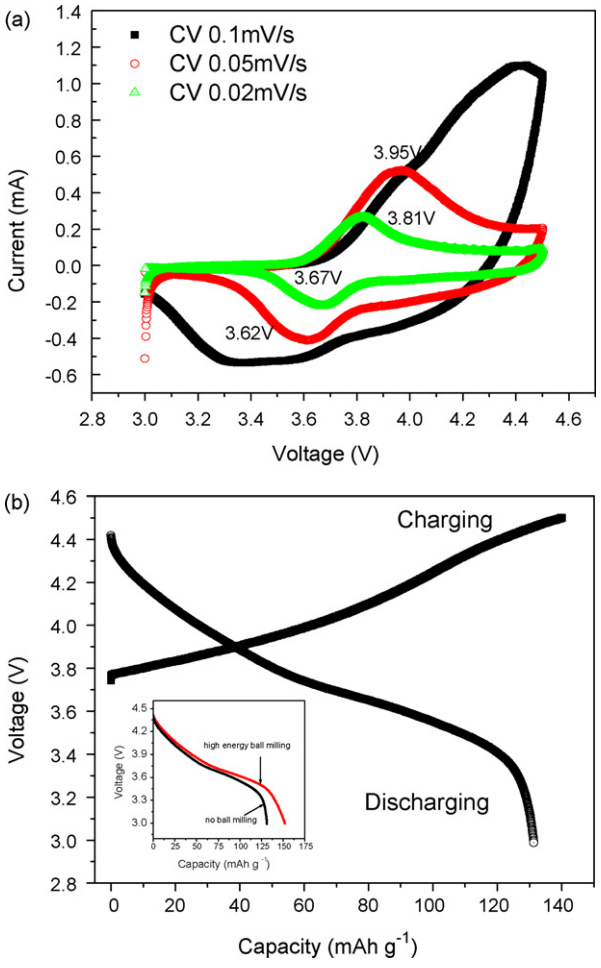

Fig. 3. $LiNi_{0.8}Co_{0.1}Mn_{0.1}O_2$ powder calcined at 900 °C for 48 h: (a) cyclic voltammograms (CV) with various scan rates for the voltage sweep range between 3 V and 4.5 V *vs.* Li and (b) First charge–discharge curves at room temperature. The inset shows the first discharge curves of two cells made from the 900 °C calcined powder: one after high-energy ball milling (HEBM) and other without HEBM.

140 mAh g^{-1} and 132 mAh g^{-1}, respectively with *C*/14 rate. The irreversible capacity loss in the first cycle was 9 mAh g^{-1}, and hence the coulombic efficiency was around 93.6% for this cathode material. The observed discharge capacity of the $LiNi_{0.8}Co_{0.1}Mn_{0.1}O_2$ was lower compared to some of the reported results [26,27]. One of the most related work by Cho et al. on $LiNi_{0.8}Co_{0.1}Mn_{0.1}O_2$ reported first cycle discharge capacity of 188 mAh g^{-1} in the voltage 3.0–4.3 V with a current of 0.1 C. This cathode material was synthesized by co-precipitation from the solution, which is having the advantage of controlling the particle size and the synthesized particle was in the nanometer range [26]. However, $LiNi_{0.6}Co_{0.2}Mn_{0.2}O_2$ synthesized by co-precipitation showed discharge capacity around 160 mAh g^{-1} and the same preparation route resulted in the discharge capacity less than 120 mAh g^{-1} also for the material calcined at temperatures >900 °C [19]. This kind of calcinations temperature dependent capacity may be due to the cationic distributions in layered structure (Li/Ni cation mixing) [28] distribution of particle sizes, etc. Also it is well known that the improved battery performances with higher reversible capacity with shorter diffusion length for Li-ion to traverse during the electrochemical interaction–deintercalation and hence lowering particle sizes in cathode materials can positively influence the capacity [29,21]. Based on the above discussion, in the present case large particles (5–8 μm) may be one of the reason for the observed low discharge capacity as compared to 188 mAh g^{-1} reported on $LiNi_{0.8}Co_{0.1}Mn_{0.1}O_2$ with particle size in nanometer range. To support this particle size hypothesis the inset of Fig. 3b shows the first discharge capacity of two cells made from the 900 °C calcined powder: for one cell the cathode was made directly from the 900 °C calcined powder (particle size ~5–8 μm) and for the other cell the cathode was made from the 900 °C calcined powder followed by a high energy ball milling step (2 h), which resulted particles in the range of 1–2 μm. Reduction in the particle size upon high energy ball milling in the present case indeed increased the discharge capacity (152 mAh g^{-1} *vs.* 132 mAh g^{-1}). This fact certainly shows that the particle size of the cathode is one of the several other important factors (like phase purity, atomic composition, cation exchange, etc.) affecting the capacity.

Structural changes in the cathode material during charge–discharge cycle are critical as the structural disorder provokes a decrease of the electronic conductivity and the ionic diffusion rate, and hence to increase the structural stability or to maintain an unchangeable conductor pathway is of great importance [30]. The *ex situ* structural investigations by XRD (Fig. 4a) were done at different stages of electrochemical process: half charge (HC), full charge (FC), half discharge (HD) and full discharge (FD). As can be seen from the figures, the starting layered structure is maintained throughout the electrochemical cycling process. The lattice parameters at the end of the discharge were comparable to the pristine values. However, in the case of intermediate stages (HC, FC and HD), a small shift in the peak positions was observed in the XRD patterns, which suggest that, the lattice parameters

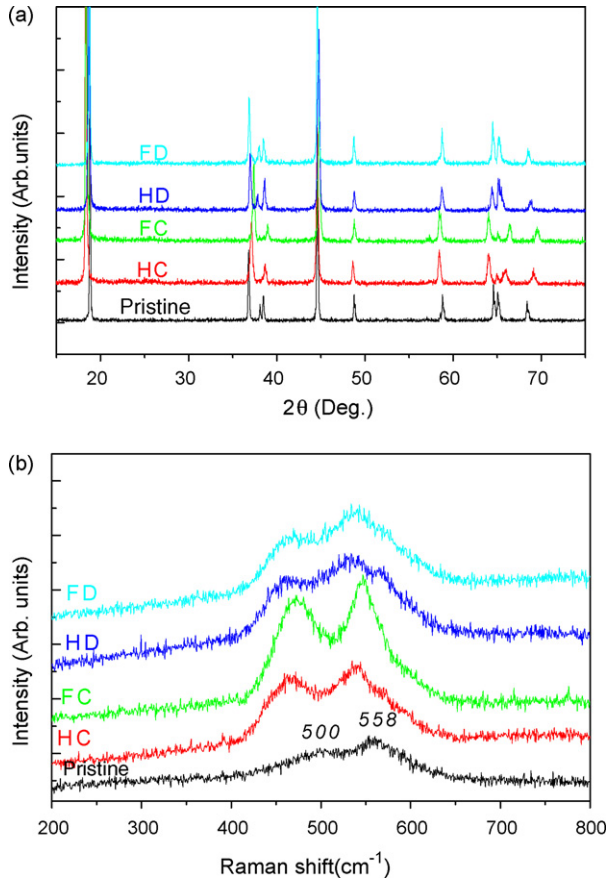

Fig. 4. Structural changes of $LiNi_{0.8}Co_{0.1}Mn_{0.1}O_2$ powder calcined at 900 °C for 48 h at various stages of charge–discharge process: (a) X-ray diffraction and (b) Raman spectra.

changes continuously during electrochemical extraction and re-insertion process. The extraction of Li from the cathode (charging), systematically reduced the '*a*' value: 2.8629 Å, 2.8308 Å, 2.8134 Å starting from the pristine, half charge to fully charged state and a reversal of trend was observed while insertion of Li to the cathode (discharging), as '*a*' value increased to 2.8429 Å and 2.8591 Å at half discharge and full discharge. In contrast, '*c*' value increased during charging and reduced during discharging. The observed values were 14.1690 Å, 14.4436 Å, 14.4762 Å, 14.2876 Å and 14.2069 Å, respectively at pristine, HC, FC, HD and FD states. This contraction and elongation of the unit cell as a result of Li (de)intercalation introduces volumetric changes in the lattice without effecting layer structure and may be reason for the observed shift in the peak positions [31].

Raman spectroscopy is very sensitive in differentiating various kinds of crystal symmetries whose atomic arrangements are closely related to one another [32,33]. Group theoretical considerations on layered lithium metal oxide with rhombohedral $R\bar{3}m$ symmetry (e.g. $LiCoO_2$) shows two Raman active modes, $A_{1g} + E_g$, whereas for the layered monoclinic $C_{2/m}$ symmetry (e.g. $LiMnO_2$), there are three Raman active modes, $2A_g + B_g$ [33]. The presence of only two bands in the Raman spectra (Fig. 4b) in our case, clearly suggests that the $R\bar{3}m$ rhombohedral symmetry for both virgin and electrochemically cycled $LiNi_{0.8}Co_{0.1}Mn_{0.1}O_2$ [32]. These bands at ~500 cm^{-1} and 560 cm^{-1} are assigned to E_g and A_{1g} modes, respectively. Thus the Raman spectra corroborated the indexing of the peaks in the XRD pattern as the rhombohedral $R\bar{3}m$ symmetry for both pristine $LiNi_{0.8}Co_{0.1}Mn_{0.1}O_2$ (Fig. 1). Theoretically, cubic spinel (e.g. $LiMn_2O_4$) predicts five Raman active modes ($A_{1g} + E_g + 3T_{2g}$). However, experimentally, presence of an intense band around 630 cm^{-1} is the signature feature of cubic spinel phase [34]. The absence of characteristic cubic spinel band ~630 cm^{-1} in both the spectra (pristine and electrochemically cycled) suggests that the prepared $LiNi_{0.8}Co_{0.1}Mn_{0.1}O_2$ is a single-phase material and the structure does not transforms into spinel after electrochemical cycling. Interestingly, the Raman spectra during the electrochemical cycling (half charge, full change and half discharge) also showed only two bands, suggestive of maintaining the layered structure throughout the charge–discharge process. However, the band position slightly changed, intensity increased with clear noticeable change in the case of fully charged state (maximum Li depletion from the cathode). This along with the case of half charge and half discharge may be due to the change in local atomic surroundings due to Li (de)intercalation, which has profound influence on the intensity and band positions rather than the structure. From the XRD and Raman results, the structural stability upon electrochemical cycling is verified with this material and hence it will be of interest in Li-ion rechargeable batteries as a cathode material.

Finally, the charge discharge profiles in the range 3–4.5 V for the first few cycles using a current of C/14 and the cycleability results of the synthesized cathode are shown in Fig. 5a and b, respectively. As mentioned before there was an irreversible capacity loss during first charge–discharge. First discharge capacity was around 132 mAh g^{-1} and discharge capacity slightly increased during initial cycles, remained almost constant till seven cycles then started to fade. At the end of 20th cycle, the capacity was around 113 mAh g^{-1}, corresponding to the capacity retentions of 86%, lower compared to the reported value, where a 92% capacity retention

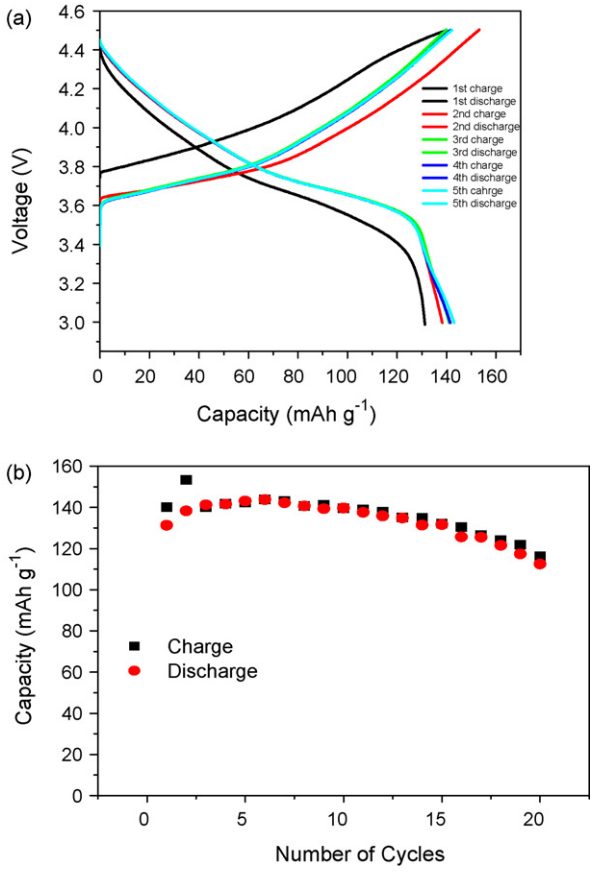

Fig. 5. Electrochemical results on $LiNi_{0.8}Co_{0.1}Mn_{0.1}O_2$ powder calcined at 900 °C for 48 h: (a) charge–discharge profiles for five cycles and (b) specific capacity *vs.* cycle number at room temperature.

was achieved even after 200 cycles [26]. Since we are sure about the structural reversibility upon electrochemical process of this material based on the X-ray and Raman studies, lowering of the particles sizes in the nanometer range, and surface modification will be considered next to improve the reversible capacity and retention. Another thing should be mentioned here that the charge discharge profiles do not change in shape with cycling and there were no distinct plateau at 4 V (characteristic of spinel phase). The absence of any 4 V plateau along the fact that the charge discharge profiles remained unchanged in shape with cycling confirms that the material did not convert into spinel upon cycling. This point again was confirmed from the Raman spectra. Raman spectra clearly distinguish the layered phase from the spinel phase. In the present case the Raman spectra of the layered phase remained almost unchanged (except little variation in band position) upon electrochemical cycling. Moreover, the characteristic spinel band ($\sim$630 cm^{-1}) did not appear in the Raman spectra upon electrochemical cycling [34]. The above two factors together show that the layered structure in the present case did not convert into spinel upon electrochemical cycling.

4. Conclusions

$LiNi_{0.8}Co_{0.1}Mn_{0.1}O_2$ cathode material has been successfully synthesized by solid-state route. Single-phase structure with layered structure (α-$NaFeO_2$ type layered structure space group $R\bar{3}m$) was obtained with calcinations in air at a temperature $\geq 900\,^{\circ}C$ for 48 h. Cyclic voltammetry showed reversibility, but the broadness of the current peak along with more separation with high scan rate suggestive of a quasi-reversible process in the system. First charge and discharge capacities in the voltage range 3.0–4.5 V were 140 mAh g^{-1} and 132 mAh g^{-1}, respectively. The structural stability and reversibility upon electrochemical cycling is verified with *ex situ* Raman scattering and X-ray diffraction studies and hence $LiNi_{0.8}Co_{0.1}Mn_{0.1}O_2$ will be of interest in Li-ion rechargeable batteries as a cathode material, if the reversible capacity and retention are improved by virtue of particle size reduction and surface modification.

Acknowledgements

Financial support from DOE (Grant #DE-FG02-01ER45868) and NASA-EPSCOR (Grant #NNX08AB12A) are acknowledged. Fruitful discussion with S.B. Majumder, J. Burgos, W. Perez and continual support from UPR materials characterization center (MCC) are also acknowledged.

References

[1] Y. Sakurai, H. Arai, S. Okada, J. Yamaki, J. Power Sources 68 (711) (1997).
[2] R. Kanno, T. Shirane, Y. Kawamoto, Y. Takeda, M. Takano, M. Ohashi, Y. Yamaguchi, J. Electrochem. Soc. 143 (1996) 2435.
[3] Y.S. Lee, C.S. Yoo, Y.K. Sun, K. Kobayakawa, Y. Sato, Electrochem. Commun. 4 (2002) 727.
[4] H. Arai, S. Okada, Y. Skurai, J.I. Yamaki, Solid State Ionics 95 (1997) 275.
[5] A.J. Paterson, A.R. Armstrong, P.G. Bruce, J. Electrochem. Soc. 151 (2004) A1552.
[6] S. Neito, S.B. Majumder, R.S. Katiyar, J. Power Sources 136 (2004) 88.
[7] A.K. Padhi, K.S. Nanjudaswamy, J.B. Goodenough, J. Electrochem. Soc. 144 (1997) 1188.
[8] C. Delmas, L. Croguennec, MRS Bull. (August) (2002) 608.
[9] S. Sivaprakash, S.B. Majumder, S. Nieto, R.S. Kartiyar, J. Power Sources 170 (2007) 433.
[10] T. Ohzuku, Y. Makimura, Chem. Lett. (2001) 642.
[11] B.J. Hwang, Y.W. Tsai, D. Carlier, G. Ceder, Chem. Mater. 15 (2003) 3676.
[12] N. Tran, L. Crouennnec, C. Jordy, P. Biensan, C. Delmas, Solid State Ionics 176 (2005) 1539.
[13] Z.X. Wang, Y.C. Sun, L.Q. Chen, X.J. Huang, J. Electrochem. Soc. 151 (2004) A914.
[14] N. Tran, L. Croguennec, C. Labrugere, C. Jordy, Ph. Biensan, C. Delmas, J. Electrochem. Soc. 153 (2006) A261.
[15] C.-C. Chen, C.-J. Wang, B.-J. Hwang, J. Power Sources 146 (2005) 626.
[16] Z. Lu, J.R. Dahn, J. Electrochem. Soc. 148 (2001) A237.
[17] N. Santander, S.R. Das, S.B. Majumder, R.S. Katiyar, Surf. Coat. Technol. 177 (2004) 60.
[18] B.J. Hwang, Y.W. Tsai, C.H. Chen, R. Santhanam, J. Mater. Chem. 13 (2003) 1962.
[19] H. Cao, Y. Zhang, J. Zhang, B. Xia, Solid State Ionics 176 (2005) 1207.
[20] J. Eom, M.G. Kim, J. Cho, J. Electrochem. Soc. 155 (3) (2008) A239.
[21] B. Wang, Y. Qiu, S. Ni, Solid State Ionics 178 (2007) 843.
[22] G.T.K. Fey, Y.Y. Lin, T.P. Kumar, Surf. Coat. Technol. 191 (2005) 68.
[23] M. Takahashi, S.-I. Tobishima, K. Takei, Y. Sakurai, Solid State Ionics 148 (2002) 283.
[24] D.Y.W. Yu, C. Fietzek, W. Weydanz, K. Donoue, T. Inoue, H. Kurokawa, S. Fujitani, J. Electrochem. Soc. 154 (2007) A253.
[25] D. Linden, T.B. Reddy, Hand book of Batteries, 3rd ed., McGraw-Hill Companies, Inc., vol. 2.22, 2001.
[26] J. Cho, T.-J. Kim, J. Kim, M. Noh, B. Park, J. Electrochem. Soc. 151 (2004) A1899.
[27] J. Cho, Y.-W. Kim, B. Kim, J.-G. Lee, B. Park, Angew. Chem. Int. Ed. Engl. 42 (2003) 1618.
[28] I. Saadoune, M. Dahbi, M. Wikberg, T. Gustafsson, P. Svedlindh, K. Edstrom, Solid State Ionics 178 (2008) 1668.
[29] A. Yamada, S.C. Chung, K. Hinokuma, J. Electrochem. Soc. 148 (2001) A224.
[30] F. Huguenin, R.M. Torresi, J. Braz. Chem. Soc 14 (2003).
[31] P.Y. Liao, J.G. Duh, H.S. Sheu, Electrochem, Solid State Lett. 10 (2007) A88.
[32] N.K. Karan, J.J. Saavedra-Arias, D.K. Pradhan, R. Melgerajo, A. Kumar, R. Thomas, R.S. Katiyar, Electrochem. Solid State Lett 11 (2008) A135.
[33] M. Inaba, Y. Iriyama, Z. Ogumi, Y. Todzuka, A. Tasaka, J. Raman Spectrosc. 28 (1997) 613.
[34] S.J. Hwang, H.S. Park, J.H. Choy, G. Campet, J. Portier, C.W. Kwon, J. Etourneau, Electrochem. Solid State Lett. 4 (2001) A213.